

This is the peer reviewed version of the following article:

Silvestre-Roig C, Fernandez P, Esteban V, Pello OM, Indolfi C, Rodriguez C, et al.  
Inactivation of Nuclear Factor- $\kappa$ B Inhibits Vascular Smooth Muscle Cell Proliferation and  
Neointima Formation. *Arterioscler Thromb Vasc Biol.* 2013;33(5):1036-45

which has been published in final form at: <https://doi.org/10.1161/ATVBAHA.112.300580>

## **Inactivation of NF- $\kappa$ B inhibits vascular smooth muscle cell proliferation and neointima formation**

Carlos Silvestre-Roig<sup>\*,\*\*</sup>; Patricia Fernández<sup>\*,\*\*,††</sup>; Vanesa Esteban<sup>\*</sup>; Óscar M. Pello<sup>\*</sup>; Ciro Indolfi<sup>‡</sup>; Cristina Rodríguez<sup>§</sup>; Ricardo Rodríguez-Calvo<sup>§</sup>; María Dolores López-Maderuelo<sup>†</sup>; Gerhard Bauriedel<sup>||</sup>; Randolph Hutter<sup>¶</sup>; Valentín Fuster<sup>\*,¶</sup>; Borja Ibáñez<sup>\*,#</sup>; Juan M. Redondo<sup>†</sup>; José Martínez-González<sup>§</sup>; Vicente Andrés<sup>\*,‡‡</sup>

<sup>\*</sup> Department of Epidemiology, Atherothrombosis and Imaging, and <sup>†</sup> Department of Vascular Biology and Inflammation, Centro Nacional de Investigaciones Cardiovasculares (CNIC), Madrid, Spain

<sup>‡</sup> Department of Medical and Surgical Sciences, Division of Cardiology, and URT CNR, University Magna Græcia, Catanzaro, Italy

<sup>§</sup> Centro de Investigación Cardiovascular, Consejo Superior de Investigaciones Científicas, Institut Català de Ciències Cardiovasculars, Instituto de Investigaciones Biomédicas Sant Pau, Barcelona, Spain

<sup>||</sup> Department of Cardiology/Heart Center, University of Bonn, Germany

<sup>¶</sup> The Zena and Michael A. Wiener Cardiovascular Institute, Mount Sinai School of Medicine, New York, US

<sup>#</sup> Cardiovascular Institute, Hospital Clínico San Carlos, Universidad Complutense, Madrid. Spain

**\*\*** Authors with equal contribution

<sup>††</sup> Present address: National Cancer Institute, NIH, 41 Library Drive, Bldg. 41, B513 Bethesda, MD 20892, US

<sup>‡‡</sup> Corresponding author: Vicente Andrés, CNIC, Melchor Fernández Almagro 3, 28029 Madrid, Spain; Phone: +34-914531200; Fax: +34-914531265; e-mail: vandres@cnic.es

**Word count of body:** 5151

**Word count of abstract:** 244

**Total number of figures and tables:** 7

**Short Title:** Role of NF- $\kappa$ B in neointimal thickening

## **ABSTRACT**

**Objective.** Atherosclerosis and restenosis are multifactorial diseases associated with abnormal vascular smooth muscle cell (VSMC) proliferation. Nuclear factor-Y (NF-Y) plays a major role in transcriptional activation of *CYCLIN B1* (*CCNB1*), a key positive regulator of cell proliferation and neointimal thickening. Here, we investigated the role of NF-Y in occlusive vascular disease.

**Approach/Results.** We performed molecular and expression studies in cultured cells, animal models and human tissues. We find up-regulation of NF-Y and cyclin B1 expression in proliferative regions of murine atherosclerotic plaques and mechanically-induced lesions, which correlates with higher binding of NF-Y to target sequences in the *CCNB1* promoter. NF-YA expression in neointimal lesions is detected in VSMCs, macrophages and endothelial cells. Platelet-derived growth factor-BB (PDGF-BB), a main inductor of VSMC growth and neointima development, induces in rat and human VSMCs the recruitment of NF-Y to the *CCNB1* promoter and augments both *CCNB1* mRNA expression and cell proliferation through extracellular signal-regulated kinase 1/2 (Erk1/2) and Akt activation. Moreover, adenovirus-mediated overexpression of a NF-YA dominant-negative mutant inhibits PDGF-BB-induced *CCNB1* expression and VSMC proliferation in vitro and neointimal lesion formation in a mouse model of femoral artery injury. We also detect NF-Y expression and DNA-binding activity in human neointimal lesions.

**Conclusions.** Our results identify NF-Y is a key downstream effector of the PDGF-BB-dependent mitogenic pathway that is activated in experimental and human vasculoproliferative diseases. They also identify NF-Y inhibition as a novel and attractive strategy for the local treatment of neointimal formation induced by vessel denudation.

**Key Words:** atherosclerosis; restenosis; VSMC proliferation; NF-Y; cyclin B1.

## INTRODUCTION

Abnormal cell proliferation is a component of the chronic inflammatory response that promotes atherosclerosis and restenosis post-angioplasty.<sup>1,2</sup> Studies with genetically-modified mice have shown that ablation of the growth suppressors p53, p27, and pRb aggravates atherosclerosis in hypercholesterolemic mice.<sup>1,3</sup> Gene therapy strategies that inhibit positive cell cycle regulators (e.g., cyclin-dependent kinases and cyclins) or upregulate growth suppressors (e.g., p16, p21, p27, p53, p57, RB2/p130) have also proved efficient at reducing neointimal thickening in animal models of atherosclerosis and restenosis.<sup>1,3</sup> Importantly, the incidence of clinical restenosis is significantly diminished by the use of stents that locally deliver antiproliferative drugs.<sup>2</sup>

Cell proliferation requires the sequential activation of cyclin-dependent kinase/cyclin complexes.<sup>4</sup> Expression of cyclin B1 (encoded by the *CCNBI* gene), which is essential for progression through mitosis and for mouse embryonic development,<sup>5</sup> is induced in the rat carotid artery model of balloon angioplasty.<sup>6</sup> Moreover, inhibition of *CCNBI* by local delivery of antisense oligonucleotides reduces neointima formation in this animal model.<sup>7</sup> Identification of the mechanisms that control *CCNBI* expression in the vasculature may therefore provide insight into the pathogenesis of atherosclerotic disease. The *CCNBI* promoter contains two CCAAT sites located at positions -17/-13 and +16/+20 relative to the transcription start site that are essential for *CCNBI* transcription during the G2/M cell cycle transition.<sup>8,9</sup> These CCAAT motifs bind nuclear factor -Y (NF-Y, also called CBF: CCAAT-binding factor), a ubiquitously expressed trimeric transcription factor formed from NF-YA, NF-YB and NF-YC subunits.<sup>10</sup> CCAAT boxes are present in approximately 25% of eukaryotic genes, and cell culture experiments demonstrate that NF-Y is required for the proliferation of fibroblasts and tumor cells.<sup>9-13</sup> However, the expression and function of NF-Y in the context of vascular pathophysiology has not been reported. Here, we hypothesized that NF-Y activation is important for the proliferative response associated with atherosclerosis and restenosis. To test this hypothesis, we performed expression and molecular studies using cultures of rat and human vascular smooth muscle cells (VSMCs), animal models (rat carotid artery balloon angioplasty and apolipoprotein E-null mouse: apoE-KO) and human atherosclerotic and restenotic tissue. We also analyzed the consequences of inactivating NF-Y on VSMC proliferation in vitro and vascular lesion formation in a mouse model of femoral artery injury.

## Results

***NF-Y activation in mechanically-injured rat arteries.*** We investigated NF-Y expression and activity in animal models of vasculoproliferative disease. First, we analyzed by immunohistochemistry the expression of NF-YA in balloon-injured rat carotid artery. We also examined the expression of cyclin B1 and PCNA, two positive regulators of cell proliferation that are induced in this animal model and contribute to neointimal thickening.<sup>6,7,14,15</sup> We found faint expression of these proteins in uninjured vessels (n=4), which was markedly increased in the lesions at early stages (7-12 days post-angioplasty, n=5) and advanced stages (14-18 days post-angioplasty, n=4) of neointimal thickening (**Fig.1A**). Quantification revealed the following percentages of immunoreactive area in early and advanced neointimal lesions: 33±7% and 29±7% for NF-YA, 28±5% and 30±10% for cyclin B1, and 37±10% and 22±7% for PCNA. Double immunofluorescence staining showed NF-YA/cyclin B1 colocalization in neointimal lesions (**Fig.1B**) and NF-YA expression in neointimal VSMCs (**Fig.1C**) and endothelial

cells (**Supplemental Fig. IA**). Moreover, double smooth muscle  $\alpha$ -actin (SMA)/NF-YA and SMA/cyclin B1 immunohistochemical analysis of consecutive sections revealed abundant expression of both NF-YA and cyclin B1 in neointimal SMA-positive VSMCs, which are the main component of mechanically-induced lesions in this animal model (**Supplemental Fig. II**).

To investigate the potential contribution of NF-Y to cyclin B1 upregulation after balloon-angioplasty, we performed EMSA with a radiolabeled probe spanning the CCAAT-box located at -17/-13 in the *CCNB1* promoter.<sup>8</sup> Uninjured rat carotid arteries exhibited no detectable NF-Y DNA-binding activity (**Fig.1D, ln.2 and 4**), but binding progressively increased at 3 (**ln.3**) and 7 (**ln.5**) days post-angioplasty. The retarded NF-Y probe was efficiently competed out by unlabeled NF-Y consensus oligonucleotide (**ln.6**), but not by NF-Y mutant (**ln.7**). The specificity of the nucleoprotein complex was further confirmed by the supershift produced by preincubation of lysates with anti-NF-YA (**ln.8**), but not with isotype-matched control antibody (**ln.9**). Mechanically-induced neointimal lesions in this animal model thus display abundant NF-YA expression and DNA-binding activity associated with the CCAAT motif at -17/-13 in the *CCNB1* promoter.

***NF-Y is a downstream effector of the platelet-derived growth factor-BB (PDGF-BB)-extracellular signal-regulated kinase 1/2 (Erk1/2)-Akt mitogenic pathway in VSMCs.*** Since PDGF-BB potently induces VSMC proliferation in vitro and is essential for neointimal hyperplasia in animal models of balloon angioplasty,<sup>16</sup> we sought to investigate whether NF-Y is a downstream effector of this cytokine. We first performed experiments with rat aortic E19P cells stimulated with PDGF-BB after starvation. qPCR and Chip assays showed that PDGF-BB significantly induced *NF-YA* mRNA expression and *in vivo* recruitment of NF-Y to the *CCNB1* promoter, reaching a maximum after 8 hours (**Fig.2A**). This was reflected in the expression of *CCNB1* mRNA and S-phase entry at 16 hours, detected by qPCR and 5'-bromo-2'-deoxyuridine (BrdU) incorporation, respectively. These three parameters returned to basal levels 32 hours after stimulation (**Fig.2A**), and were all significantly blunted by pretreatment of E19P cells with either U0126 (inhibitor of Erk1/2 activation) or the Akt inhibitor X, but not the p38 inhibitor SB203580 (**Fig.2B**). U0126 and Akt inhibitor X similarly reduced PDGF-BB-dependent NF-Y binding to the *CCNB1* promoter, *CCNB1* mRNA expression and cell proliferation in human VSMCs (**Fig.2C**).

***Effects of NF-Y inactivation on primary VSMCs and endothelial cells.*** We next investigated whether NF-Y activity is involved in *CCNB1* expression and proliferation in primary rat and human VSMCs. Cells were infected with either AdGFP, which encodes GFP, or Ad(GFP+NF-YAdn), which gives rise to a bicistronic mRNA encoding both GFP and a dominant-negative mutant NF-YA13m29 that inhibits NF-Y activity.<sup>17</sup> Ad(GFP+NF-YAdn)-infected rat VSMCs overexpressed NF-YA13m29 (**Fig.3A**) and exhibited reduced NF-Y DNA-binding activity (**Fig.3B, ln.4 versus 2 and 3**). Moreover, compared with control AdGFP, Ad(GFP+NF-YAdn) impaired FBS-dependent upregulation of *CCNB1* mRNA and BrdU incorporation in rat VSMCs (**Fig.3C**). Infection of human VSMCs with Ad(GFP+NF-YAdn) also reduced PDGF-BB-dependent *CCNB1* mRNA expression and proliferation (**Fig.3D**). We also found a slight but significant increase in apoptosis in Ad(GFP+NF-YAdn)-infected rat VSMCs compared with Ad-GFP-infected controls (**Supplemental Fig. IIIA**). In marked contrast, NF-YA inactivation did not affect proliferation and apoptosis in primary mouse aortic endothelial cells (**Supplemental Fig. IB**).

***Inhibition of NF-Y activity reduces neointimal thickening induced by arterial denudation.*** To assess the effects of inhibiting NF-Y on neointimal thickening in vivo, we performed gene therapy studies using a mouse model of femoral artery wire-injury. Immediately after injury, Ad(GFP+NF-YAdn) or control AdGFP was infused intraluminally and arteries were exposed to the virus for 20 minutes. Arteries were removed 9 days after denudation. Effective gene delivery was demonstrated by the presence of GFP-immunoreactive cells in arteries infected with either viral vector, but not in control (uninfected, uninjured) vessels (**Fig.4A**). To examine the effect of NF-YAdn expression on DNA-binding activity, we performed EMSAs with arterial lysates and a probe containing the NF-Y binding site at -17/-13 in the *CCNB1* promoter. Control experiments using lysates from AdGFP-infected arteries revealed a retarded nucleoprotein complex that was abrogated with either unlabeled NF-Y consensus oligonucleotide or anti-NF-YA antibody, but not with NF-Y mutant oligonucleotide or anti-CREBII (**Fig.4B**). In agreement with the results in the rat carotid artery angioplasty model (**Fig.1D**), NF-Y DNA-binding activity was undetectable in uninjured mouse femoral arteries and was markedly upregulated in injured vessels (**Fig.4C, ln.2 versus 3**). Importantly, ectopic expression of NF-YAdn significantly reduced injury-induced DNA-binding activity (**Fig.4C, ln.3 versus 4**) and inhibited neointimal thickening (47% reduction in intima-to-media ratio,  $p=0.002$ ) without significantly affecting medial area (**Fig.4D**).

***NF-Y activation in mouse atherosclerotic lesions.*** We also studied the role of NF-Y in native atherosclerosis by performing immunohistochemical analysis in atherosclerosis-prone apoE-KO mice and wild-type controls (**Fig.5A**). Expression of NF-YA, cyclin B1 and the proliferation marker Ki67 was faint in cross-sections of non-atherosclerotic aortas from wild-type and apoE-KO mice fed control diet. In marked contrast, atherosclerotic lesions of fat-fed apoE-KO mice contained areas that were immunoreactive for these proteins (NF-YA:  $30\pm 4\%$ ; cyclin B1:  $25\pm 2\%$ ; Ki67:  $9\pm 2\%$ ), which were also expressed in spontaneously-formed lesions in older apoE-KO mice fed control chow (not shown). Double immunofluorescence experiments in aorta from fat-fed apoE-KO mice revealed abundant NF-YA expression in neointimal macrophages and VSMCs, which are the predominant cells in the atheroma (**Fig.5B**). Moreover, these cells express cyclin B1, as revealed by double immunohistochemical analysis (**Supplemental Fig. IV**). We also find NF-YA expression in endothelial cells lining atherosclerotic lesions (**Supplemental Fig. IC**).

We next performed EMSA using the NF-Y binding site at -17/-13 in the *CCNB1* promoter, which revealed increased NF-Y DNA-binding activity in the atherosclerotic aortic arch and thoracic aorta of apoE-KO mice (**Fig.5C, ln.3 and 5**) compared with non-atherosclerotic tissue from wild-type controls (**Fig.5C, ln.2 and 4**). Specificity of the retarded nucleoprotein complexes was demonstrated by competition and supershift assays (**Fig.5C, ln.6-10**).

***NF-Y activation in human restenotic and atherosclerotic lesions.*** To address the clinical relevance of our findings, we carried out pilot immunohistochemistry studies to analyze NF-YA expression in human restenotic and atherosclerotic vessels. In human restenotic coronary artery tissue obtained by percutaneous directional atherectomy, NF-YA was detected in 9 out of 10 specimens analyzed, with varying degrees of expression among the different patients (**Fig.6A**). The analysis of consecutive sections of human restenotic tissue revealed regions with abundant NF-YA and cyclin B1 expression (**Fig.6B**).

We also detected NF-YA in 7 out of 8 human atherosclerotic coronary artery specimens (**Fig.6C**). The analysis of consecutive sections showed regions with abundant NF-YA and cyclin B1 expression (**Fig.6D**), and double immunofluorescence studies revealed NF-YA expression in

neointimal VSMCs and endothelial cells lining the lesions (**Supplemental Fig. V**). As shown in **Fig.6E**, human atherosclerotic coronary arteries (**ln. 12-16**) also exhibited increased NF-Y DNA-binding activity compared with control internal mammary arteries (**ln. 2-6**) and coronary arteries (**ln. 7-11**) ( $7.6 \pm 1.3$  fold increase,  $p < 0.001$ ). Specificity of the retarded nucleoprotein complexes was demonstrated by competition and supershift assays (**Fig.6F**).

## DISCUSSION

Cyclin B1 is essential for cell cycle progression and its genetic disruption in the mouse causes embryonic lethality.<sup>5</sup> Under normal conditions, cyclin B1 expression is tightly regulated to ensure that it accumulates appreciably only during the G2/M cell cycle transition.<sup>9</sup> Aberrantly high levels of cyclin B1 throughout the cell cycle as a result of deregulated gene transcription is associated with excessive cell proliferation in several human cancers.<sup>18</sup> Moreover, expression of cyclin B1 is induced in balloon-injured rat carotid artery,<sup>6</sup> and local delivery of antisense oligonucleotides against *CCNBI* inhibits neointima formation in a rat carotid artery model of balloon angioplasty.<sup>7</sup> While these results highlight the role of *CCNBI* in promoting mechanically-induced neointimal thickening, the mechanisms that regulate its expression in vascular cells remain elusive. In the present study, we hypothesized that induction of the heterotrimeric transcription factor NF-Y, acting through increasing *CCNBI* expression, is important for neointimal thickening. We focused on NF-YA because NF-Y activity is mainly controlled through changes in NF-YA protein expression and post-translational modifications.<sup>10</sup> By combining cell culture experiments and studies with animal models and human specimens, we provide evidence that NF-Y plays an important role in inducing cyclin B1 expression and VSMC proliferation in atherosclerotic and restenotic lesions (**Fig.7**). We have shown that balloon angioplasty in the rat carotid artery causes a temporally and spatially coordinated expression of NF-YA and cyclin B1 in neointimal lesions with proliferative activity. Using this model and a mouse model of arterial wire injury, we also find a marked upregulation of NF-Y DNA-binding activity in the damaged vessel wall. Likewise, expression of NF-YA, cyclin B1 and the proliferation marker Ki67 is upregulated in atheromata of apoE-KO mice, and this is accompanied by a marked increase in NF-Y DNA-binding activity compared with non-atherosclerotic tissue. NF-Y-dependent induction of cyclin B1 expression may also contribute to neointimal cell proliferation in patients, since our pilot studies revealed expression of both proteins in human atherosclerotic and restenotic tissue, as well as increased NF-Y DNA binding to its target sequence in the *CCNBI* promoter in atherosclerotic coronary arteries compared with control vessels. Future studies are thus warranted to further investigate the expression and activity of NF-Y in a larger set of occlusive vascular lesions.

Our studies revealed expression of NF-YA in neointimal VSMCs and macrophages and in endothelial cells lining neointimal lesions. Interestingly, we find that adenovirus-mediated NF-Y inhibition does not affect endothelial cell proliferation and apoptosis in vitro. It will be important to ascertain whether NF-Y exerts cell cycle- and apoptosis-independent actions in vascular endothelial cells and/or neointimal macrophages. For example, given that NF-Y regulates myeloid differentiation,<sup>19</sup> studies are warranted to investigate its role in macrophage inflammatory response, including cytokine production, phagocytic activity and lipoprotein uptake. Future studies should also address whether NF-Y expression/activity in vascular cells and macrophages is regulated by lipid-modulating and anti-

inflammatory strategies recently developed to treat atherosclerosis,<sup>20</sup> and to ascertain whether these new therapies may cooperate with anti-NF- $\kappa$ B approaches.

Consistent with previous studies in fibroblasts and tumor cells that demonstrated reduced *CCNB1* expression and cell proliferation upon inhibition of NF- $\kappa$ B DNA-binding activity,<sup>11-13, 21</sup> we find that NF- $\kappa$ B inhibition in cultures of VSMCs reduces mitogen-induced *CCNB1* expression and cell proliferation. The in vivo relevance of these results is further highlighted by the observation that intraluminal delivery of adenovirus encoding the dominant-negative NF- $\kappa$ B mutant inhibits NF- $\kappa$ B DNA-binding activity and neointima development in a mouse model of arterial injury. Cell proliferation occurs mainly at early stages of vascular remodeling induced by mechanical injury.<sup>3</sup> We found no differences in neointimal Ki67 immunoreactivity in arteries infected with Ad(GFP+NF- $\kappa$ BAdn) at the time point analyzed for lesion quantification (**Supplemental Fig. IIIB**), which corresponds to an advanced stage of disease progression. These results suggest that NF- $\kappa$ B inhibits VSMC proliferation during the first days after vessel denudation. Given that apoptotic cell death also occurs in mechanically-injured arteries, we also analyzed the effect of NF- $\kappa$ B inactivation on apoptosis. Whilst we found a modest increase in apoptosis of primary VSMCs infected with Ad(GFP+NF- $\kappa$ BAdn), NF- $\kappa$ B inactivation did not affect apoptosis in mouse femoral neointimal lesions and in primary endothelial cell cultures.

Studies in animal models of atherosclerosis and arterial denudation have conclusively demonstrated that neointimal thickening is significantly dependent upon PDGF signaling, and both PDGF-BB and its receptor PDGFR- $\beta$  are expressed in atherosclerotic and restenotic lesions in experimental animals and humans.<sup>16</sup> It is now recognized that the Erk1/2 and Akt signaling cascades are downstream effectors of PDGF in VSMCs<sup>22-24</sup> that stimulate neointimal thickening after vascular injury.<sup>25, 26</sup> The results of our qPCR and ChIP studies demonstrate that PDGF-BB induces NF- $\kappa$ B expression and its recruitment to the endogenous *CCNB1* promoter in rat and human VSMCs, and this is followed by increased *CCNB1* mRNA expression and cell proliferation. These responses to PDGF-BB are impaired upon treatment with pharmacological inhibitors of either Erk1/2 or Akt or by NF- $\kappa$ B dominant-negative mutant overexpression. Collectively, our results identify NF- $\kappa$ B as an important downstream mediator in the PDGF-BB-Erk1/2-Akt-dependent signaling cascade that contributes to neointimal thickening through the induction of *CCNB1* expression and VSMC proliferation (**Fig. 7**). It is therefore possible that inhibiting NF- $\kappa$ B would offer a more specific and safer strategy than targeting its upstream effectors Akt and Erk1/2, which control multiple physiological processes that are essential for the maintenance of cellular and organismal homeostasis (e.g., differentiation, motility, apoptosis, autophagy, angiogenesis, metabolism, and protein synthesis).<sup>27, 28</sup> In this regard, the pyrrolobenzodiazepine-polyamide conjugate GWL-78 has been shown to displace NF- $\kappa$ B from several CCAAT motifs within promoters of cell cycle genes, and to block fibroblast proliferation.<sup>13</sup> Preclinical studies in large animal models are thus warranted to explore the efficacy of GWL-78 at preventing neointimal thickening.

In summary, our results show that the transcription factor NF- $\kappa$ B is induced in experimental and human atherosclerosis and restenosis. We also find that adenovirus-mediated inactivation of NF- $\kappa$ B attenuates PDGF-BB-induced VSMC proliferation in vitro and the development of neointimal lesions in a mouse model of vascular injury. We therefore propose that NF- $\kappa$ B is an attractive novel target for intervention in atherosclerosis and restenosis as well as other vascular-remodeling diseases that display VSMC proliferation (e.g., transplant atherosclerosis and pulmonary hypertension).



## **ACKNOWLEDGMENTS**

We are grateful to colleagues who generously provided reagents (R. Mantovani for NF-Y and GFP expression vectors; J. Font de Mora for anti-cyclin B1 antibody; C. Shanahan for E19P cells). We are also indebted to M. Hamczyk, P. Molina and S. Laudato for help with qPCR and immunofluorescence microscopy, M. J. Andrés-Manzano for figure preparation, and S. Bartlett for English editing.

## **SOURCES OF FUNDING**

This study was funded by the Spanish Ministry of Economy and Competiveness (MINECO) (grants SAF2010-16044, SAF2009-11949), Instituto de Salud Carlos III (ISCIII) (grants RD12/0042/0021, RD12/0042/0028, RD12/0042/0053), and the Dr. Léon Dumont Prize 2010 by the Belgian Society of Cardiology (to V.A.). P.F. received salary support from ISCIII and C.S. from Fundación Mario Losantos del Campo and Fundación Ferrer para la Investigación. O.M.P. and R.R.-C. hold a Juan de la Cierva contract (MINECO). V.E. is an investigator of the Sara Borell program (CD06/00232). The CNIC is supported by MINECO and Pro-CNIC Foundation.

## **DISCLOSURES**

None.

## REFERENCES

1. Fuster JJ, Fernández P, González-Navarro H, Silvestre C, Abu Nabah YN, Andrés V. Control of cell proliferation in atherosclerosis: Insights from animal models and human studies. *Cardiovasc Res.* 2010;86:254-264
2. Wessely R. New drug-eluting stent concepts. *Nat Rev Cardiol.* 2010;7:194-203
3. Andrés V. Control of vascular cell proliferation and migration by cyclin-dependent kinase signalling: New perspectives and therapeutic potential. *Cardiovasc Res.* 2004;63:11-21
4. Ekholm SV, Reed SI. Regulation of G(1) cyclin-dependent kinases in the mammalian cell cycle. *Curr Opin Cell Biol.* 2000;12:676-684
5. Santamaría D, Ortega S. Cyclins and CDKs in development and cancer: Lessons from genetically modified mice. *Front Biosci.* 2006;11:1164-1188
6. Braun-Dullaeus RC, Mann MJ, Seay U, Zhang L, von Der Leyen HE, Morris RE, Dzau VJ. Cell cycle protein expression in vascular smooth muscle cells in vitro and in vivo is regulated through phosphatidylinositol 3-kinase and mammalian target of rapamycin. *Arterioscler Thromb Vasc Biol.* 2001;21:1152-1158
7. Morishita R, Gibbons GH, Kaneda Y, Ogihara T, Dzau VJ. Pharmacokinetics of antisense oligodeoxyribonucleotides (cyclin B1 and CDC 2 kinase) in the vessel wall in vivo: Enhanced therapeutic utility for restenosis by hvj-liposome delivery. *Gene.* 1994;149:13-19
8. Farina A, Manni I, Fontemaggi G, Tiainen M, Cenciarelli C, Bellorini M, Mantovani R, Sacchi A, Piaggio G. Down-regulation of cyclin B1 gene transcription in terminally differentiated skeletal muscle cells is associated with loss of functional CCAAT-binding NF-Y complex. *Oncogene.* 1999;18:2818-2827
9. Porter LA, Donoghue DJ. Cyclin B1 and CDK1: Nuclear localization and upstream regulators. *Prog Cell Cycle Res.* 2003;5:335-347
10. Mantovani R. The molecular biology of the CCAAT-binding factor NF-Y. *Gene.* 1999;239:15-27
11. Hu Q, Lu JF, Luo R, Sen S, Maity SN. Inhibition of CBF/NF-Y mediated transcription activation arrests cells at G2/M phase and suppresses expression of genes activated at G2/M phase of the cell cycle. *Nucleic Acids Res.* 2006;34:6272-6285
12. Hu Q, Maity SN. Stable expression of a dominant negative mutant of CCAAT binding factor/NF-Y in mouse fibroblast cells resulting in retardation of cell growth and inhibition of transcription of various cellular genes. *J Biol Chem.* 2000;275:4435-4444
13. Kotecha M, Kluza J, Wells G, O'Hare CC, Forni C, Mantovani R, Howard PW, Morris P, Thurston DE, Hartley JA, Hochhauser D. Inhibition of DNA binding of the NF-Y transcription factor by the pyrrolbenzodiazepine-polyamide conjugate GWL-78. *Mol Cancer Ther.* 2008;7:1319-1328
14. Morishita R, Gibbons GH, Ellison KE, Nakajima M, Zhang L, Kaneda Y, Ogihara T, Dzau VJ. Single intraluminal delivery of antisense CDC2 kinase and proliferating-cell nuclear antigen oligonucleotides results in chronic inhibition of neointimal hyperplasia. *Proc Natl Acad Sci USA.* 1993;90:8474-8478
15. Wei GL, Krasinski K, Kearney M, Isner JM, Walsh K, Andrés V. Temporally and spatially coordinated expression of cell cycle regulatory factors after angioplasty. *Circ Res.* 1997;80:418-426
16. Raines EW. PDGF and cardiovascular disease. *Cytokine Growth Factor Rev.* 2004;15:237-254

17. Mantovani R, Li XY, Pessara U, Hooft van Huisjduijnen R, Benoist C, Mathis D. Dominant negative analogs of NF- $\kappa$ B. *J Biol Chem*. 1994;269:20340-20346
18. Egloff AM, Vella LA, Finn OJ. Cyclin b1 and other cyclins as tumor antigens in immunosurveillance and immunotherapy of cancer. *Cancer Res*. 2006;66:6-9
19. Sjin RM, Krishnaraju K, Hoffman B, Liebermann DA. Transcriptional regulation of myeloid differentiation primary response (MyD) genes during myeloid differentiation is mediated by nuclear factor  $\kappa$ B. *Blood*. 2002;100:80-88
20. Weber C, Noels H. Atherosclerosis: Current pathogenesis and therapeutic options. *Nat Med*. 2011;17:1410-1422
21. Gurtner A, Manni I, Fuschi P, Mantovani R, Guadagni F, Sacchi A, Piaggio G. Requirement for down-regulation of the CCAAT-binding activity of the NF- $\kappa$ B transcription factor during skeletal muscle differentiation. *Mol Biol Cell*. 2003;14:2706-2715
22. Choudhury GG, Karamitsos C, Hernandez J, Gentilini A, Bardgette J, Abboud HE. PI-3-kinase and MAPK regulate mesangial cell proliferation and migration in response to PDGF. *Am J Physiol*. 1997;273:F931-938
23. Choudhury GG, Mahimainathan L, Das F, Venkatesan B, Ghosh-Choudhury N. c-Src couples PI 3 kinase/Akt and MAPK signaling to PDGF-induced DNA synthesis in mesangial cells. *Cell Signal*. 2006;18:1854-1864
24. Deuse T, Koyanagi T, Erben RG, Hua X, Velden J, Ikeno F, Reichenspurner H, Robbins RC, Mochly-Rosen D, Schrepfer S. Sustained inhibition of epsilon protein kinase C inhibits vascular restenosis after balloon injury and stenting. *Circulation*. 2010;122:S170-178
25. Mitra AK, Agrawal DK. In stent restenosis: Bane of the stent era. *J Clin Pathol*. 2006;59:232-239
26. Muslin AJ. MAPK signalling in cardiovascular health and disease: Molecular mechanisms and therapeutic targets. *Clin Sci (Lond)*. 2008;115:203-218
27. Mattmann ME, Stoops SL, Lindsley CW. Inhibition of Akt with small molecules and biologics: Historical perspective and current status of the patent landscape. *Expert Opin Ther Pat*. 2011;21:1309-1338
28. Mendoza MC, Er EE, Blenis J. The Ras-ERK and PI3K-mTOR pathways: Cross-talk and compensation. *Trends Biochem Sci*. 2011;36:320-328

## **SIGNIFICANCE**

Excessive vascular smooth muscle cells (VSMC) proliferation contributes to neointima formation during atherosclerosis and restenosis post-angioplasty. Here, using rodent models and human specimens, we show that the transcription factor NF- $\kappa$ B is activated in neointimal lesions and is a key downstream mediator of the PDGF-BB-Erk1/2-Akt signaling cascade that contributes to VSMC proliferation. Adenovirus-mediated overexpression of a NF- $\kappa$ B dominant-negative mutant inhibits VSMC but not endothelial cell proliferation in vitro, and attenuates neointimal thickening in a mouse model of wire injury. Targeting NF- $\kappa$ B might offer a more specific and safer strategy for limiting in-stent restenosis than inhibition of its upstream effectors, which control multiple homeostatic processes. A candidate drug is the anti-NF- $\kappa$ B compound GWL-78, which inhibits cell-cycle gene expression and proliferation. Preclinical studies are thus warranted to assess the efficacy of anti-NF- $\kappa$ B strategies in vascular-remodeling disorders involving VSMC hyperplasia, such as atherosclerosis, restenosis, transplant atherosclerosis and pulmonary hypertension.

## FIGURE LEGENDS

**Fig.1. Upregulation of NF-YA and cyclin B1 expression and NF-Y DNA-binding activity in balloon-injured rat carotid artery.** (A) Representative examples of immunohistochemical analysis in early (10 d) and advanced (18 d) stages of neointimal thickening. Black and white arrowheads: internal and external elastic lamina, respectively. Bar: 50  $\mu$ m. (B) Double confocal immunofluorescence microscopy of neointimal lesion. Bar: 10  $\mu$ m. (C) Confocal immunofluorescence microscopy of neointimal lesion showing smooth muscle  $\alpha$ -actin (SMA), NF-YA and nuclei (DAPI). Arrowheads: NF-YA/SMA-positive cells. Bar: 20  $\mu$ m. (D) EMSA with arterial lysates and a radiolabeled NF-Y binding site containing the CCAAT-box at -17/-13 in the human *CCNB1* promoter (NF-Ycons). Competition assays (ln.6, 7) were carried out with unlabeled NF-Ycons or mutated (NF-Ymut) oligonucleotide. For supershift assays (ln.8, 9), extracts were preincubated with antibodies.

**Fig.2. PDGF-BB induces NF-Y binding to the *CCNB1* promoter, cyclin B1 expression and VSMC proliferation via Erk1/2 and Akt.** Serum-starved rat E19P cells (A, B) and primary human VSMCs (C) stimulated with PDGF-BB to perform Chip, qPCR, and BrdU incorporation assays (n=3-4). Results are expressed relative to unstimulated cells (=1). When indicated, cells were treated with SB203580 (p38MAPK inhibitor), U0126 (Erk1/2 inhibitor) or Akt inhibitor X. PDGF-BB was added and cells were collected after 8 hours (Chip) and 16 hours (qPCR, BrdU incorporation). (C) Cells were cultured with or without U0126 and Akt inhibitor X. PDGF-BB was added and cells were collected at 12 hours (Chip) and 24 hours (qPCR, BrdU incorporation).\*: p<0.05, \*\*: p<0.01, \*\*\*: p<0.001, versus vehicle.

**Fig.3. NF-Y inactivation in VSMCs reduces *CCNB1* expression and cell proliferation.** Primary rat (A, B, C) and human (D) VSMCs were infected with AdGFP (encoding GFP) or Ad(GFP+NF-YAdn) (which gives rise to a bicistronic mRNA encoding both GFP and NF-YA13m29 dominant-negative mutant). (A) Western blot of nuclear and cytoplasmic fractions. Nuclear lamin A/C was analyzed to control for fraction purity. (B) EMSA using nuclear extracts and NF-Ycons probe. Ln.5, 6: competition with 50-fold molar excess of unlabeled NF-Ycons or NF-Ymut oligonucleotide. (C) Serum-starved cells stimulated with 20% FBS. *CCNB1* mRNA (qPCR) and proliferation (BrdU incorporation) analyzed after 16 and 24 hours of stimulation, respectively. (D) Serum-starved cells stimulated with PDGF-BB. *CCNB1* mRNA and proliferation analyzed after 24 hours of stimulation. Results of qPCR are expressed relative to unstimulated cells (=1, discontinuous line). The percentage of BrdU-immunoreactive cells was determined in GFP-positive cells and the results are expressed relative to AdGFP (=1).

**Fig.4. NF-Y inhibition by local adenoviral transduction of NF-YAdn attenuates neointimal thickening in a mouse femoral artery injury model.** All studies were performed with tissue extracted 9 days after wire injury. (A) Representative immunohistochemistry of GFP expression. The tunica media is delimited by discontinuous lines (red: internal elastic lamina; black: external elastic lamina). No Ab: negative control lacking primary antibody. All images are at the same magnification (Bar: 20  $\mu$ m). (B) EMSA with NF-Ycons probe and lysates from AdGFP-infected arteries (pool of 14 arteries). (C) EMSAs using NF-Ycons probe and lysates from control (uninjured, uninfected) and injured arteries infected with either AdGFP or Ad(GFP+NF-YAdn) (pools of 4, 14 and 12 arteries, respectively). Only retarded nucleoprotein complexes are shown in representative autoradiographs. Graph: quantification of retarded complex intensities averaged from 7 independent EMSAs (relative to uninjured=1). \*: p<0.05, \*\*: p<0.001, versus uninjured. (D) Quantification of medial and intimal area,

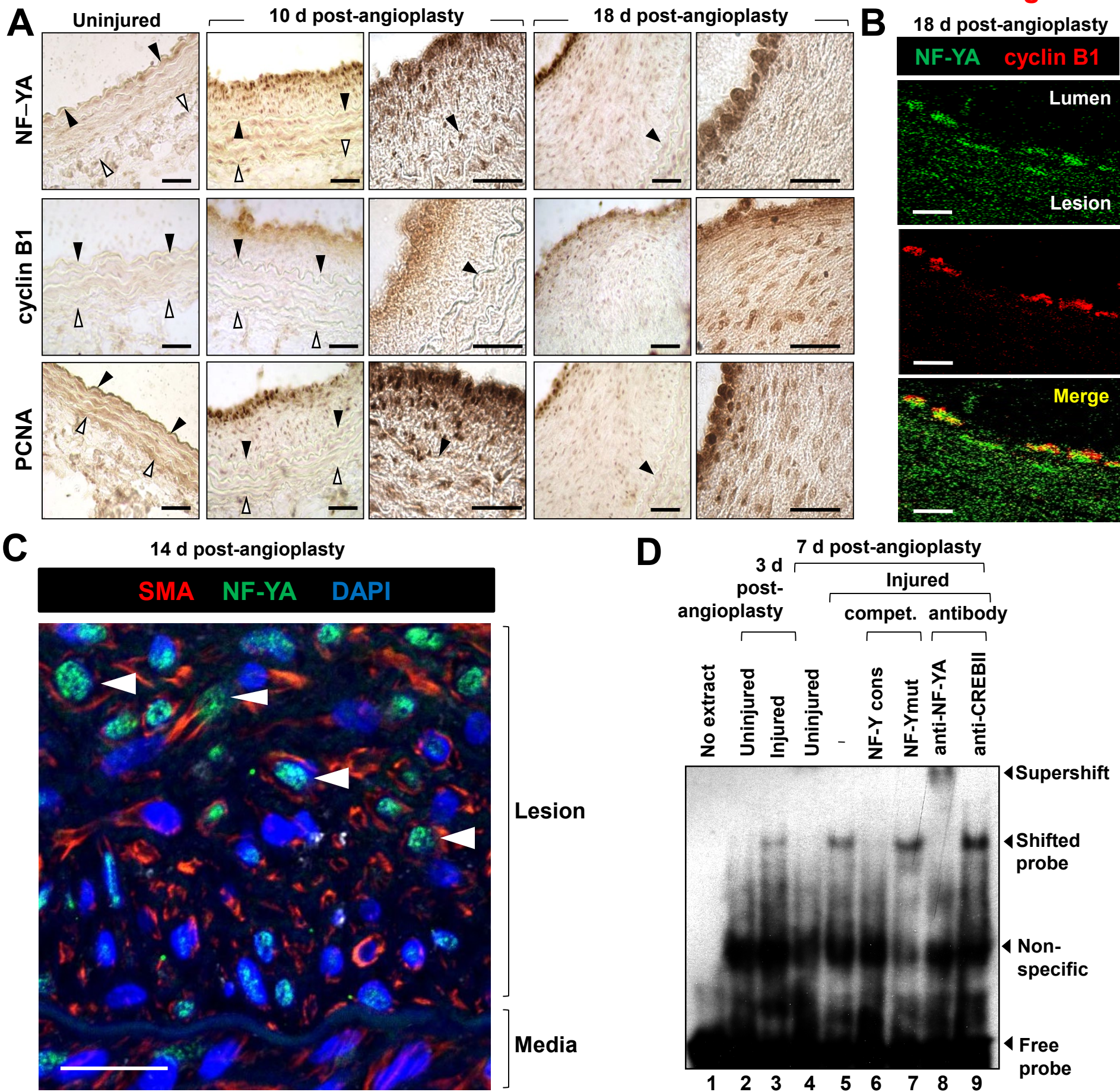
intima-to-media, and stenosis. Representative photomicrographs of hematoxylin-eosin and Masson's trichrome staining. Bar: 100  $\mu$ m.

**Fig.5. Upregulation of NF-YA and cyclin B1 expression and NF-Y DNA-binding activity in mouse atherosclerosis.** (A) Immunohistochemistry in aorta of wild-type and apoE-KO mice. The photomicrographs show representative examples of the indicated number of mice. Black and white arrowheads: internal and external elastic lamina, respectively. (B) Confocal immunofluorescence microscopy of aortic atheroma from fat-fed apoE-KO mice to visualize NF-YA, Mac3 (macrophages), and SMA (VSMCs). Arrowheads point to NF-YA/Mac3- or NF-YA/SMA-positive cells. The dashed line indicates the internal elastic lamina. (C) EMSA using aortic lysates from 11-month-old mice fed control diet and radiolabeled NF-Y consensus probe. Competition assays were carried out with unlabeled NF-Ycons or NF-Ymut. For supershift assays (ln.9, 10), extracts were preincubated with antibodies.

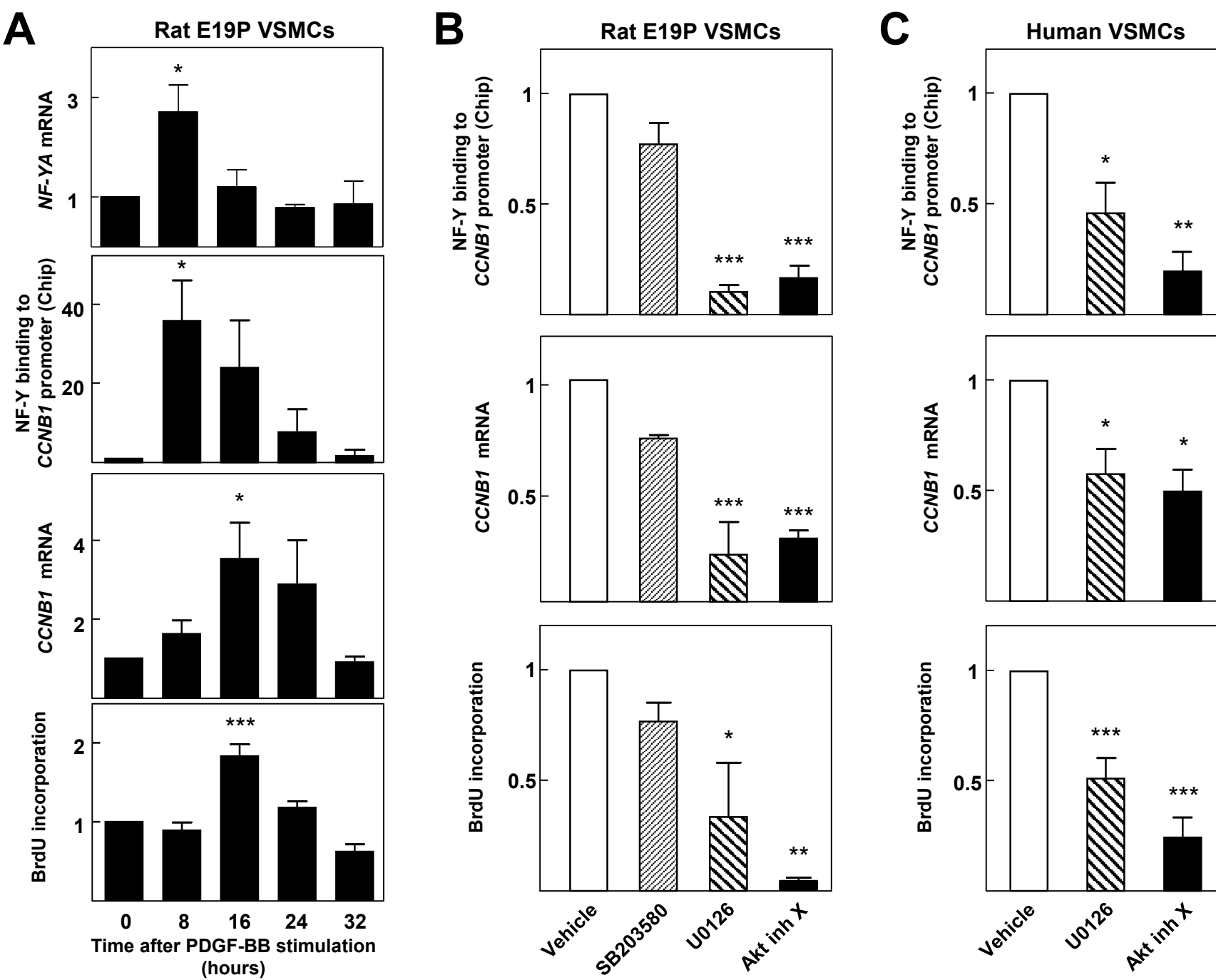
**Fig.6. Expression of NF-YA and cyclin B1 and NF-Y DNA-binding activity in human coronary restenosis and atherosclerosis.** (A) Immunohistochemical analysis was performed in tissue obtained by atherectomy after a first intervention (PTCA: percutaneous transluminal coronary angioplasty; Ath: atherectomy). LAD: left anterior descending; RCA: right coronary artery; RCx: Ramus circumflexus. NF-YA expression was graded by two independent observers (observer 1 rating/observer 2 rating) according to a semiquantitative scale (ND: not detected; +: weak; ++: moderate; +++: high). The photomicrographs show examples of NF-YA staining in different specimens. (B) Consecutive sections from the same restenotic specimen illustrating regions with low and abundant NF-YA and cyclin B1 expression. (C, D) Immunohistochemical analysis was performed in human coronary arteries with varying degrees of atherosclerosis according to American Heart Association criteria: early (type I and II), intermediate (type III), and advanced (type IV-VI) lesion. The extent of NF-YA staining was graded by two independent observers (observer 1 rating/observer 2 rating) according to a semiquantitative scale (Interm.: Intermediate; Adv.: Advanced; ND: not detected; +: weak; ++: moderate; +++: extensive). The photomicrographs correspond to two magnifications of consecutive sections from the same specimen showing a region with abundant NF-YA and cyclin B1 expression. (E) EMSA performed with human arterial lysates (five patients for each condition) and radiolabeled NF-Y consensus probe (NF-Y binding site at -17/-13 in human *CCNBI*). The graph shows band intensities of the retarded DNA-protein complexes relative to control coronary artery (=1). (F) Competition assays in atherosclerotic coronary artery were carried out with a 100-fold molar excess of unlabeled NF-Ycons or NF-Ymut oligonucleotide. For supershift assays, lysates were preincubated with antibodies.

**Fig.7. Proposed role of NF-Y in neointimal hyperplasia.** NF-Y is a downstream effector of the PDGF-BB-Erk1/2-Akt signaling pathway that contributes to *CCNBI* expression, VSMC proliferation and neointimal formation.



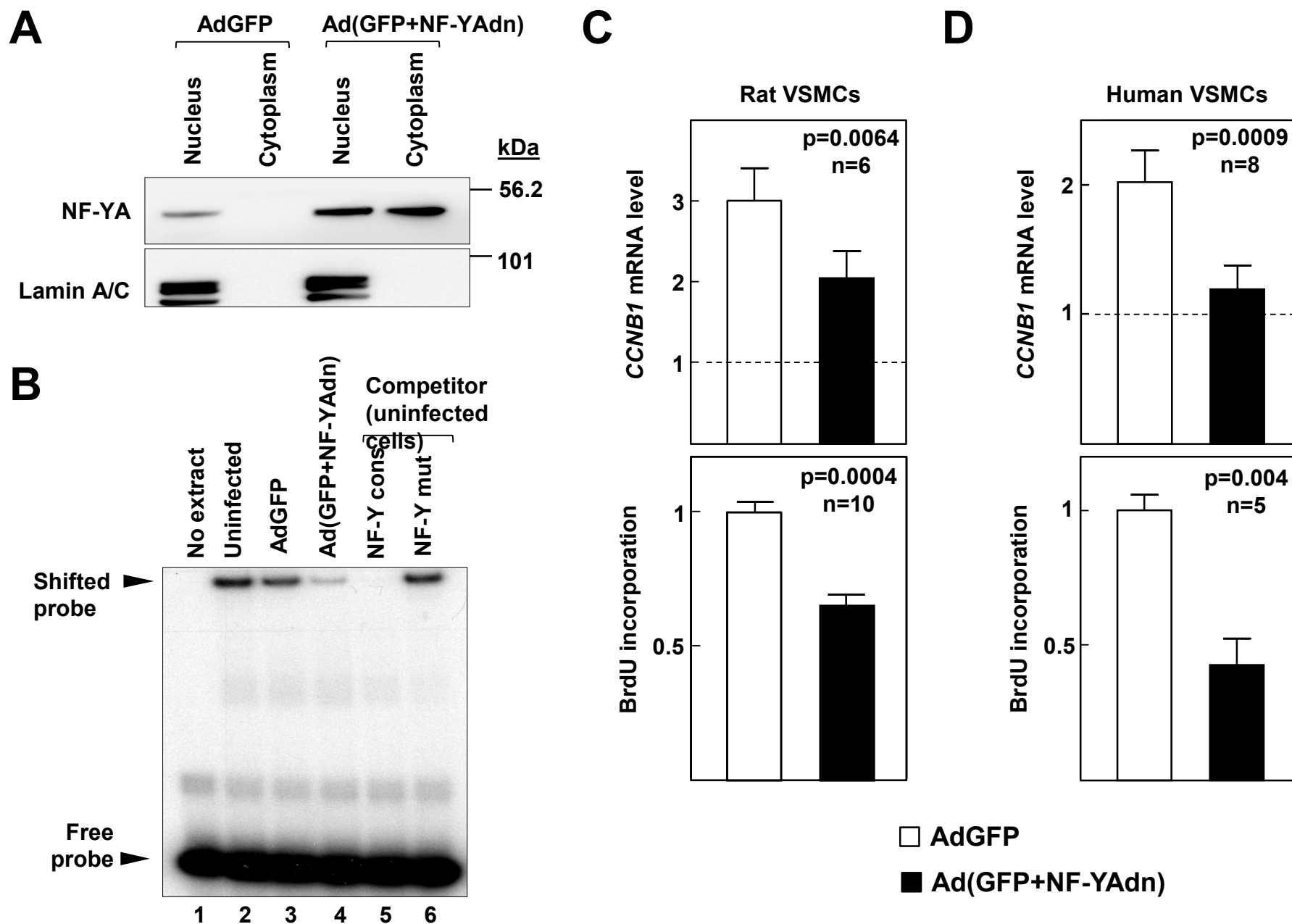
**Figure 1**

**Figure 2**

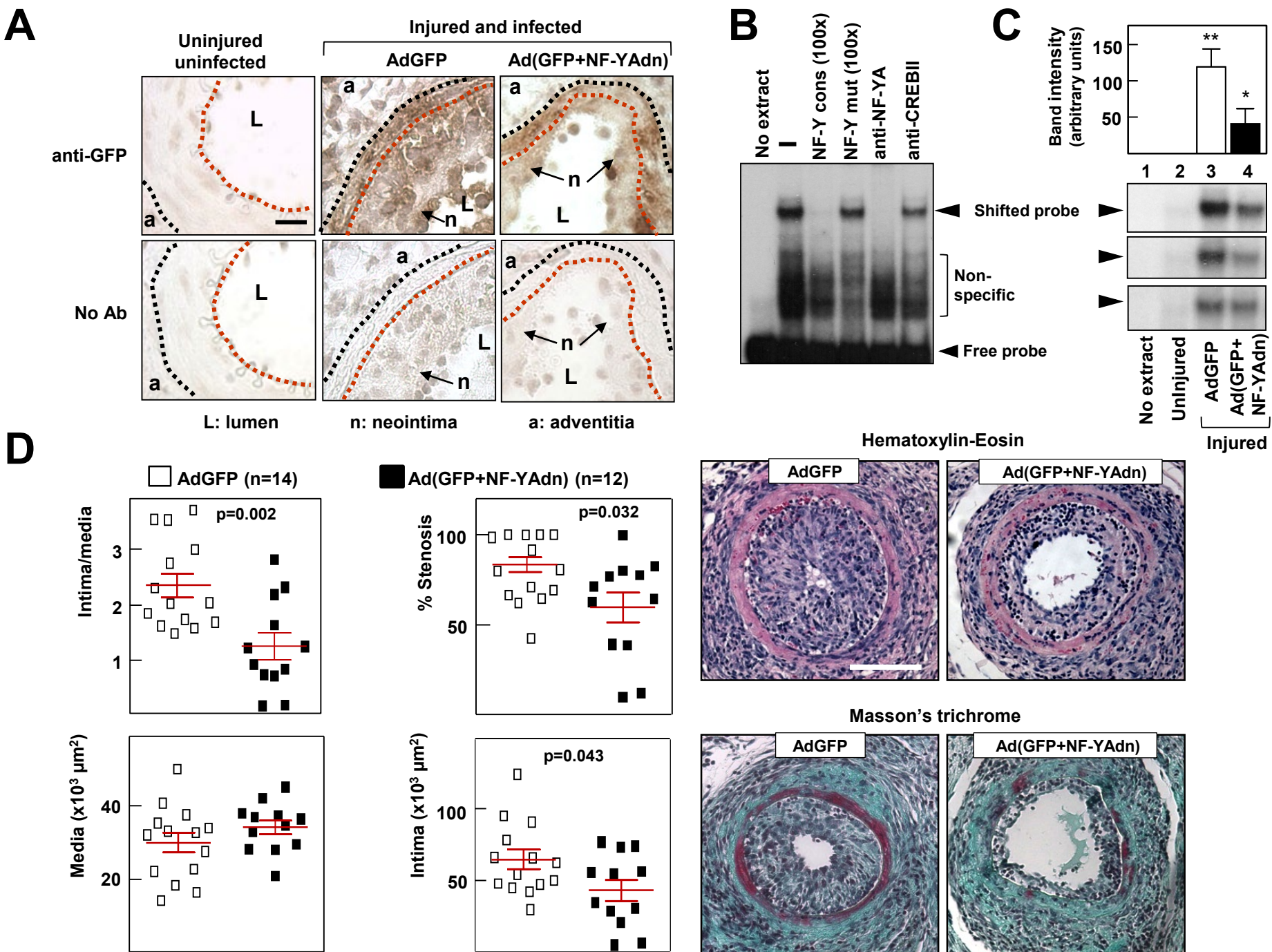




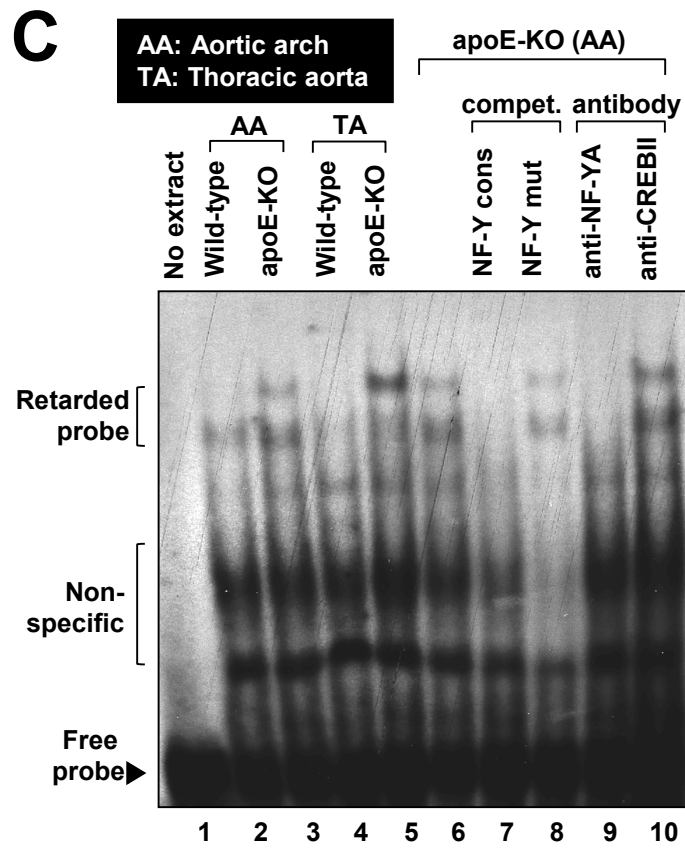
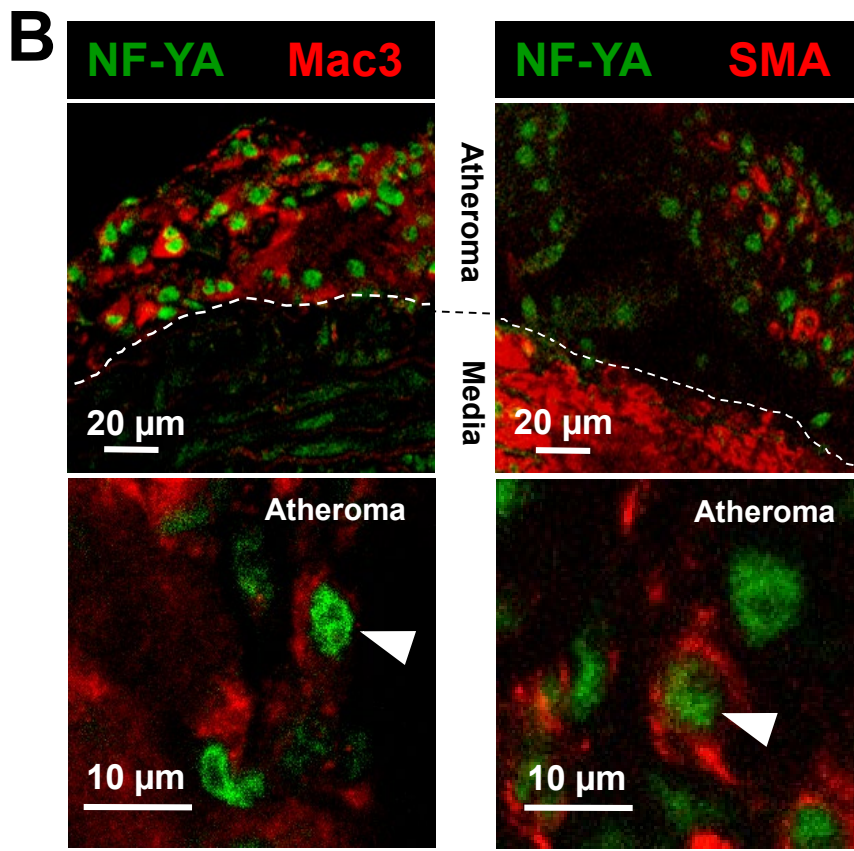
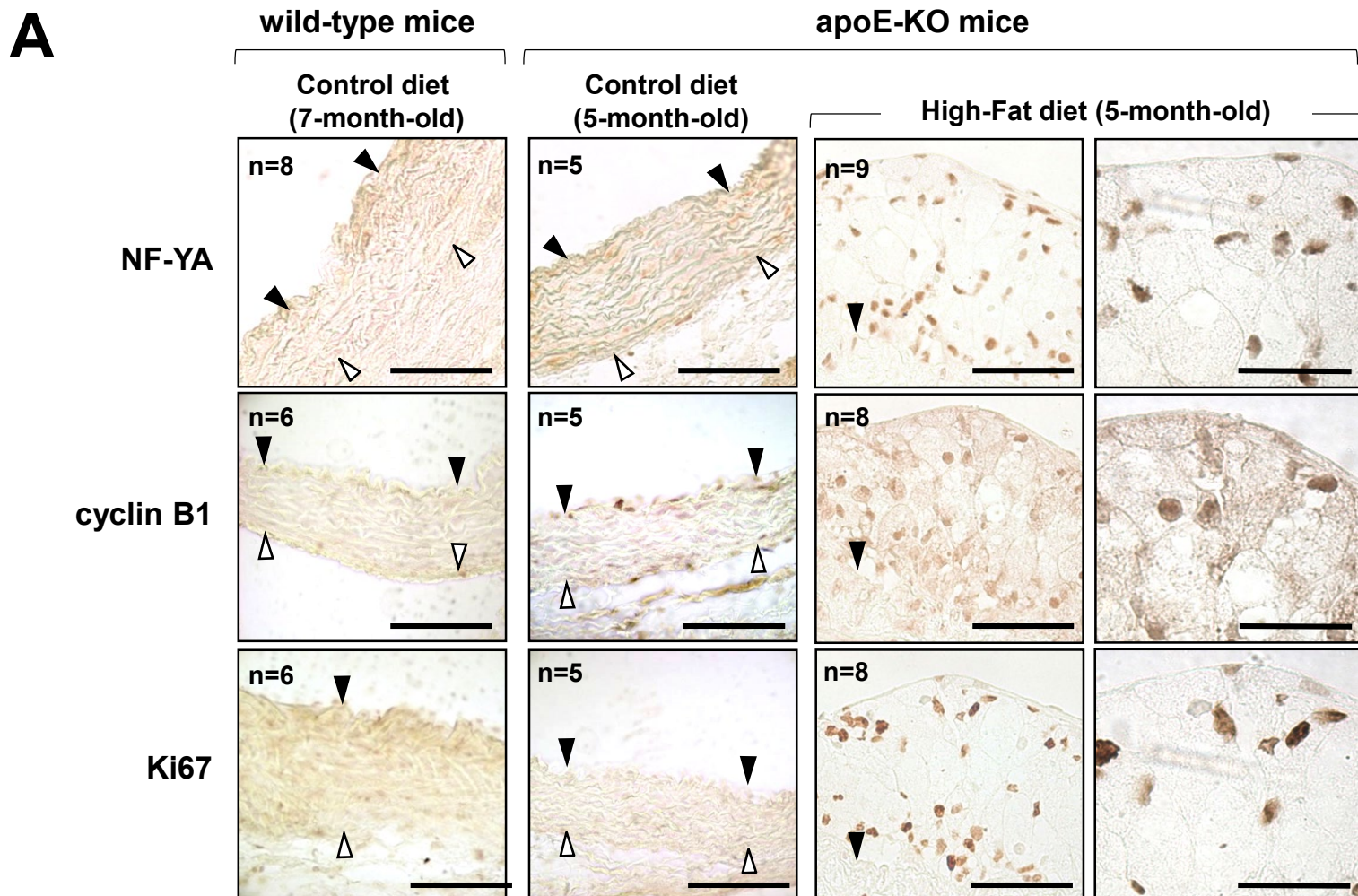
**Figure 3**



**Figure 4**









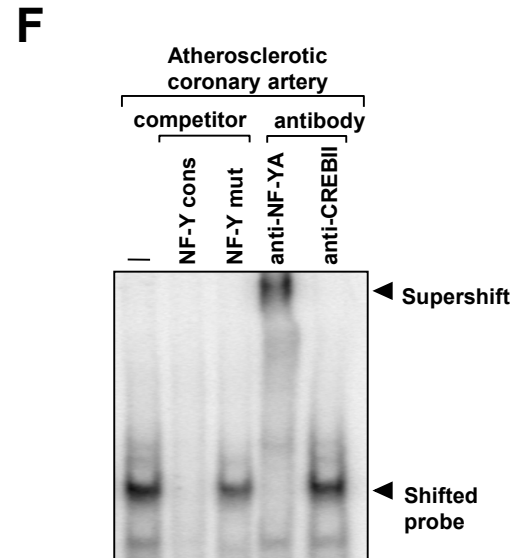
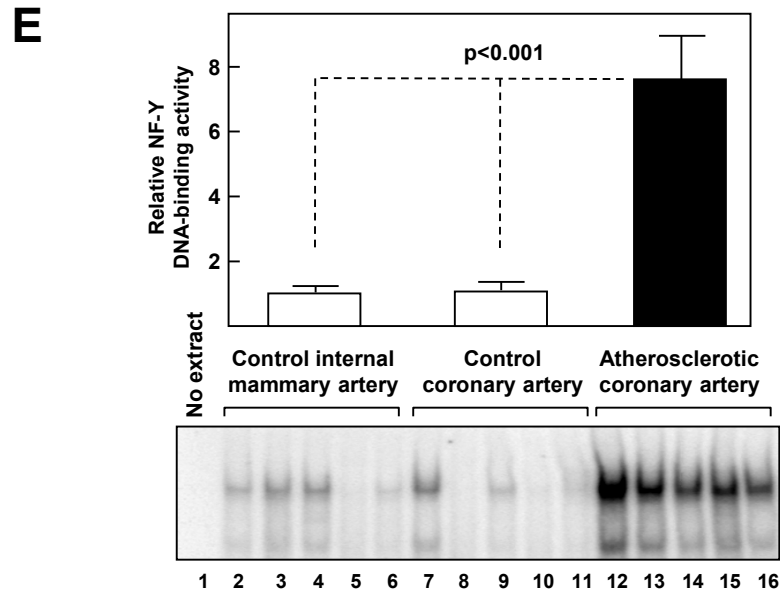
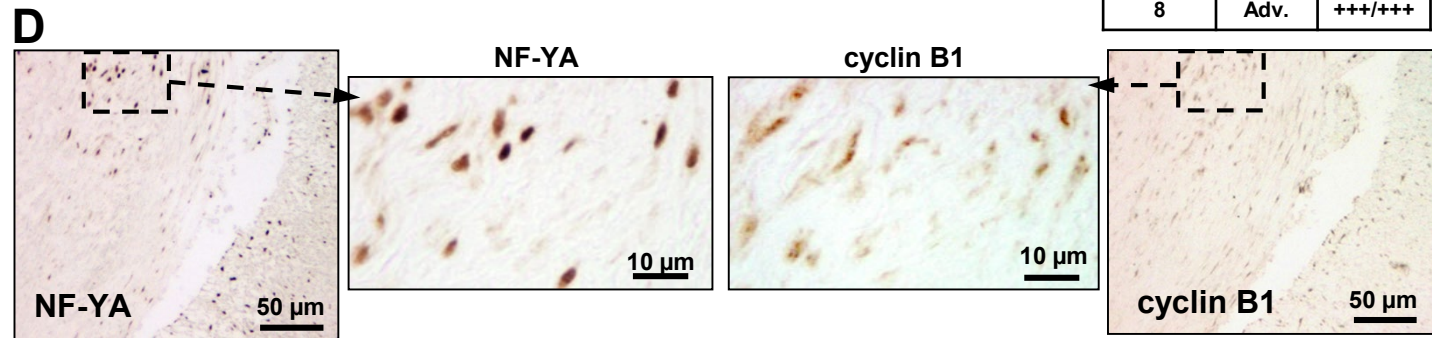
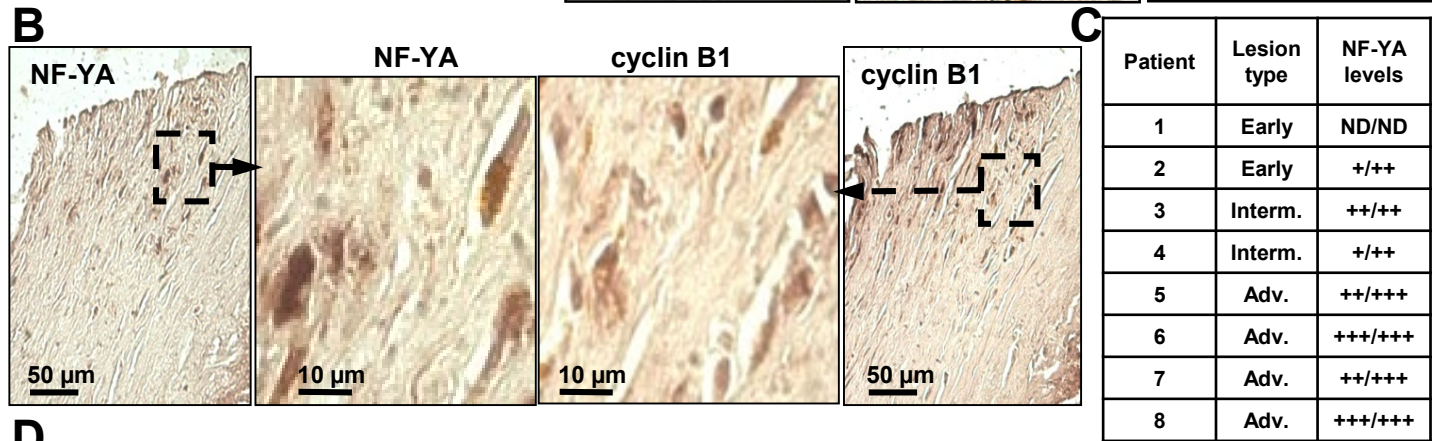
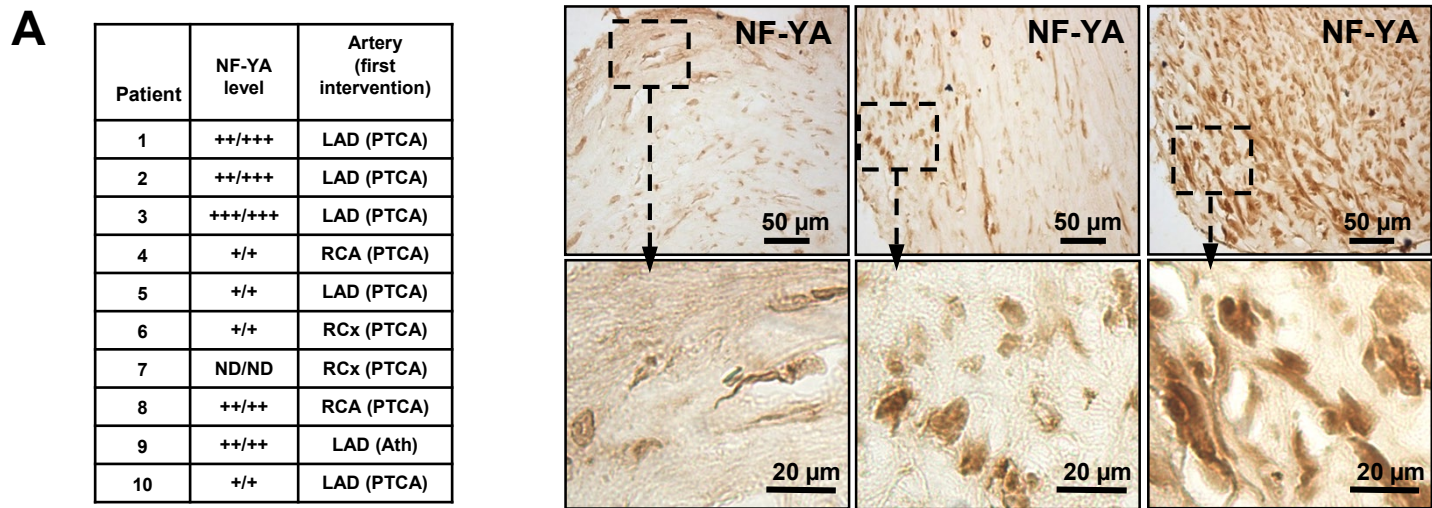
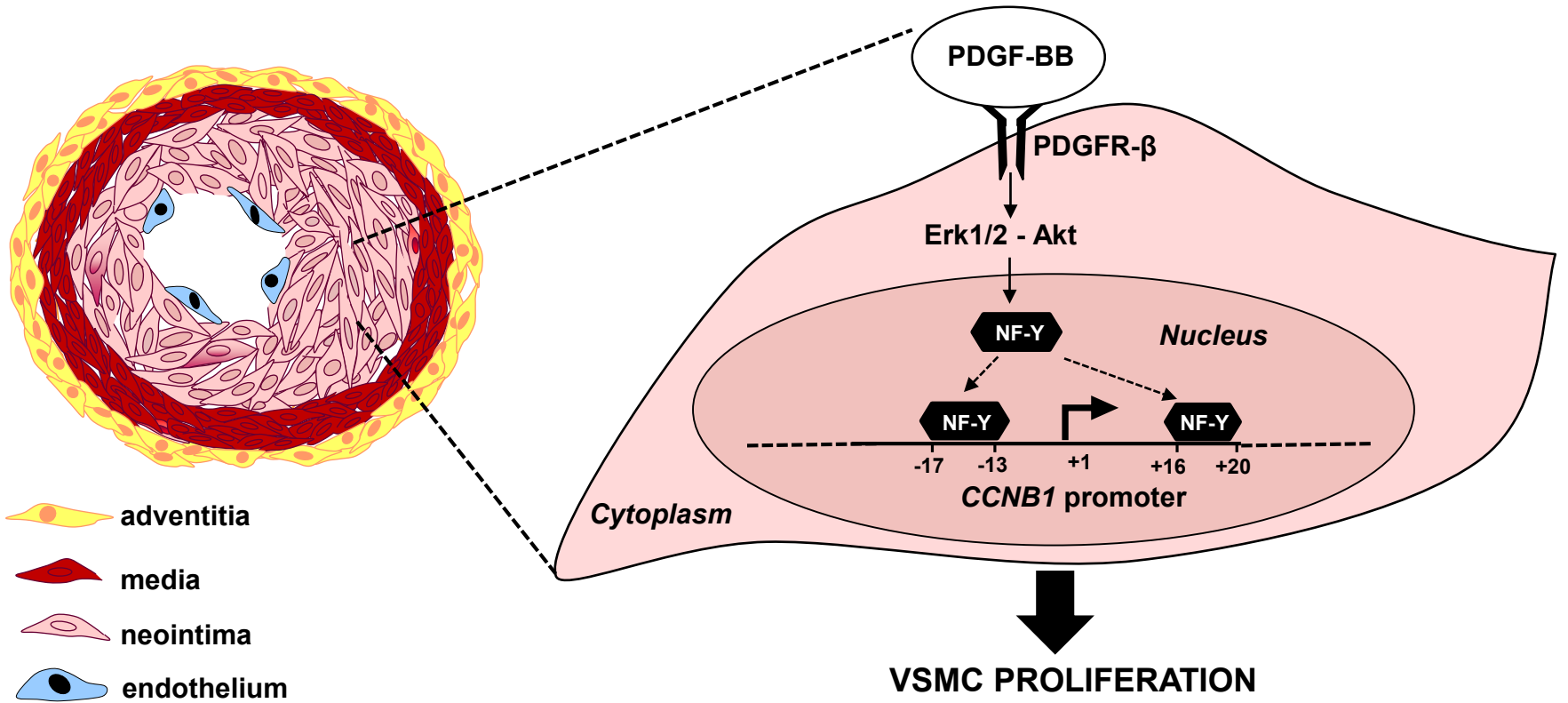


**Figure 7**



## MATERIALS AND METHODS

**Animal models.** Care of animals was in accordance with institutional guidelines and regulations and animal procedures received approval from the Ethics Committee. Mice deficient for apolipoprotein E (apoE-KO)<sup>1</sup> and wild-type controls (both C57BL/6J, Charles River, Lyon, France) were maintained on standard chow (2.8% fat; Panlab, Barcelona, Spain) or fed for two months an atherogenic diet containing 10.8% total fat and 0.75% cholesterol (S8492-E010, Ssniff, Germany).

Balloon-angioplasty was performed in the carotid artery of Wistar rats (400 g, 14-week-old) as previously described.<sup>2</sup> Rats were anesthetized by intramuscular injection with ketamine (100 mg/kg, Ketalar, Parker Davis, Milan, Italy) and xylazine (5 mg/kg, Rompun, Bayer AG, Leverkusen, Germany). A 2F Fogarty balloon catheter (Edwards Laboratory, Santa Ana, CA) was then introduced through the external carotid artery, the balloon was inflated at 1.5 atmospheres and drawn towards the arteriotomy site three times to denude the artery.

Endoluminal injury to the common femoral artery of 2-month-old male mice (C57BL/6J) was performed by 1 passage of a 0.25 mm diameter guidewire (Advanced Cardiovascular Systems). The guidewire was introduced and advanced through the femoral artery until reaching the aortic bifurcation, where a temporary ligation was placed to stop blood flow and allow incubation with adenovirus produced as previously described.<sup>3</sup> Control mice were infected with adenovirus expressing green fluorescent protein (AdGFP) and experimental mice with adenovirus expressing both GFP and the dominant-negative nuclear factor-YA13m29 mutant (Ad(GFP+NF-YAdn))<sup>4</sup> (a gift from R. Mantovani, Italy). After placing the temporary ligation, the guidewire was withdrawn, virus (10  $\mu$ L containing 1,000 pfu/mL) was delivered intraluminally using a cannula, and a permanent ligation was made at the arteriotomy site. After 20 min, the distal ligation was removed to restore blood flow through the injured vessel segment. Mice were sacrificed 9 days after injury and tissue was cleaned and fixed in 4% of paraformaldehyde or snap-frozen for subsequent studies. Fixed tissue was paraffin-embedded and 5- $\mu$ m sections were cut through the entire injured segment. Sections were stained with hematoxylin-eosin and those free of thrombus were used for anatomical studies. An investigator blinded to treatment measured stenosis and intima and media area using ImageJ software (National Institutes of Health, Bethesda, MD). Stenosis was calculated using the following equation:

$$\% \text{ stenosis} = 100 \times [\text{Intimal area} / (\text{Lumen area} + \text{Intimal area})].$$

For each injured vessel, results represent the average from all sections analyzed. The procedures to assess protein expression and NF-Y DNA-binding activity are described below. Apoptosis was analyzed using the In Situ Cell Death Detection Kit (11684795910, Roche, Applied Science, Indianapolis, IN).

**Human arterial tissue.** Sampling and processing of coronary artery specimens obtained by percutaneous directional atherectomy performed in patients with stable angina attributed to the presence of restenotic lesions after previous balloon angioplasty (9 patients) or atherectomy (1 patient) have been previously described.<sup>5</sup> Coronary and internal mammary arteries were collected from patients undergoing heart transplant and coronary artery bypass-graft surgery, respectively (Hospital de la Santa Creu i Sant Pau, Barcelona, Spain). Atherosclerotic and non-atherosclerotic coronary arteries were from coronary artery disease (CAD) and non-CAD patients, respectively. Immediately after surgical excision, arteries were dissected, immersed in cell maintenance media, and cleaned of connective tissue and fat. Specimens for expression studies were fixed overnight in 4% paraformaldehyde/PBS (pH 7.4), paraffin embedded and sectioned with a microtome (Jung RM2055, Leica, Solms, Germany). The presence of atherosclerotic lesions was evaluated by Masson's trichrome or hematoxylin/eosin staining.<sup>6</sup> The studies were approved by the ethics committees and conducted according to the Declaration of Helsinki.

**Electrophoretic mobility shift assay (EMSA).** To investigate NF-Y DNA-binding activity, freshly-isolated arteries were snap-frozen in liquid nitrogen and stored at -80°C until the preparation of protein extracts. EMSA was performed as described<sup>7</sup> using 25 µg of total protein from arterial lysates,<sup>8</sup> or 5 µg of nuclear extract from vascular smooth muscle cells (VSMCs).<sup>9</sup> To generate the radiolabeled NF-Y consensus probe, a double-stranded 27-mer oligonucleotide spanning the NF-Y DNA-binding site at position -17/-13 in the human CYCLIN B1 promoter (Forward: 5'-CCGCAGCCGCCAATGGGAAGGGAGTGA-3'; Reverse: 5'-TCACTCCCTTCCCATTGGCGGCTGCGG-3'; CCAAT motif underlined) was labeled with [<sup>32</sup>P]dATP using polynucleotide kinase (New England Biolabs, Ipswich, MA) and purified on a Sephadex G-50 column (GE healthcare, UK). For competition experiments, binding reactions contained the indicated fold-excess of unlabeled NF-Y consensus or NF-Y mutant, in which the CCAAT motif is disrupted (Forward: 5'-CCGCAGCCGTAATGGGAAGGGAGTGA-3'; Reverse: 5'-TCACTCCCTTCCCATTAAACGGCTGCGG-3'; mutations underlined). For supershift assays, lysates were preincubated for 25 min with 1 µg of anti-NF-YA or anti-CREBII (sc-10779X and sc-22800X, respectively, Santa Cruz Biotechnology, Santa Cruz, CA) before adding probe. Binding reactions were resolved by electrophoresis at 4°C under non-denaturing conditions (5% polyacrylamide/0.5X TBE buffer). Gels were dried and autoradiographed and the intensity of the retarded bands was quantified with Metamorph and ImageQuant v5.2 (GE healthcare).

**Immunostaining.** Human tissues were fixed as indicated above and animal tissues with 4% paraformaldehyde/PBS. After sectioning and antigen retrieval with citrate buffer (10

mM, pH 6.0), specimens were blocked with 5% goat serum/phosphate buffered saline. Primary antibodies were anti-NF- $\kappa$ B (1/500-1/2000, sc-10779X), anti-cyclin B1 (1/100, sc-752), anti-proliferating-cell nuclear antigen (1/200, sc-7907) from Santa Cruz Biotechnology, anti-Ki67 (MAD-000310QD, SP6, Vitro, Madrid, Spain), anti-Mac3 (1/500, SC-19991), phosphatase alkaline-conjugated anti-smooth muscle  $\alpha$ -actin (SMA) (1/50, A5691, Sigma, St. Louis, MO) and anti-GFP (1/100, ab290, Abcam, Cambridge, MA). After extensive washes, sections from rat and mouse atherosclerotic vessels were incubated with horseradish peroxidase-conjugated goat anti-rabbit (sc-2313, Santa Cruz Biotechnology) or with phosphatase alkaline-conjugated anti-rat (ab7098, Abcam) secondary antibodies and sections from human specimens or mouse femoral arteries with biotinylated anti-rabbit antibodies (atherosclerotic samples: BA-1000, Vector Labs., Burlingame, CA; murine and human restenotic samples: 111-066-003, Jackson ImmunoResearch, Suffolk, UK). Immunocomplexes conjugated to horseradish peroxidase were detected with Vectastain Elite ABC reagent (PK6100, Vector) and DAB substrate (AbD Serotec, Dusseldorf, Germany). Immunocomplexes conjugated to phosphatase alkaline were detected with Warp Red Chromogen Kit (WR806, Biocare Medical, Concord, CA).

Immunostaining in rodent histological sections was quantified by computer-assisted morphometric analysis using ImageJ software (National Institutes of Health) and immunoreactive area is presented as a percentage of the total neointimal area. The extent of immunostaining in human histological sections was graded by two independent observers according to a semiquantitative scale (ND: not detected; +: weak; ++: moderate; +++: high).

Primary antibodies for confocal immunofluorescence were anti-NF- $\kappa$ B (1/2000, sc-10779X), anti-Mac3 (1/500, SC-19991) and anti-cyclin-B1 (1/100, sc-245) from Santa Cruz Biotechnology, and Cy3-conjugated anti-SMA (1/1000, C6198, Sigma). Secondary antibodies were Alexa Fluor 488- or 555-conjugated goat anti-rabbit, Alexa Fluor 488-conjugated goat anti-mouse, and Alexa Fluor 633-conjugated goat anti-rat (A11034, A21429, A11029 and A21094, respectively, Invitrogen, Breda, The Netherlands). For endothelial cell staining, tissue was incubated with biotinylated-isolectin B4 (1/20, L2140, Sigma) in PBS containing 1% Triton X-100, 0.1 mM  $\text{CaCl}_2$ , 0.1 mM  $\text{MgCl}_2$  and 0.1 mM  $\text{MnCl}_2$ , followed by incubation with Alexa Fluor 647-conjugated streptavidin (S21374, Invitrogen). Images were acquired with a laser microscope (TCS/SP2, Leica, Wetzlar, Germany, or A1R, Nikon, Melville, NY) and image colocalization was evaluated with MetaMorph (Danaher Corporate Office, Downingtown, PA).

**Cell culture and adenoviral infection.** Cells were maintained at 37°C in 5%  $\text{CO}_2$ . Rat VSMCs were obtained from thoracic aortas of Wistar-Kyoto rats by collagenase digestion.<sup>10</sup> E19P cells (gift from C. Shanahan, University of Cambridge, UK) were obtained from explant cultures of embryonic day 19 aorta from Fischer rats. Cells were cultured in DMEM medium (Invitrogen) supplemented with heat-inactivated fetal bovine



serum (FBS, Sigma) (10% and 20% FBS for E19P and primary rat VSMCs, respectively) and 1% penicillin/streptomycin (Gibco, Invitrogen). For isolation of mouse aortic endothelial cells (mAECs), segments of abdominal and thoracic aortas were dissected and processed as previously described.<sup>11</sup> Explants were not disturbed during the first days. After outgrowth of adherent cells, a positive selection was performed using anti-ICAM-2 antibody (553326, clone 3C4, BD Biosciences), which yielded a population of endothelial cells with a >95% purity. mAECs were cultured in DMEM:F12, 1:1 Mixture 12-719F (BE12-719F, Lonza, Basel, Switzerland) supplemented with 10% FBS, heparin (0.1 mg/ml, H3393, Sigma), Endothelial Cell Growth Supplement (ECGF, 50 µg/ml, 354006, Becton Dickinson, Franklin Lakes, NJ), 1% penicillin/streptomycin (Gibco, Invitrogen), glutamine, 10 mM Hepes and fungizone. VSMCs from human coronary arteries were obtained as previously described<sup>12</sup> and were maintained with 20% FBS/2% human serum in M199 medium (Gibco, Invitrogen).

Cells were infected for 6 hours with AdGFP or Ad(GFP+NF-YAdn) (see above) at a multiplicity of infection of 200 in serum-free DMEM supplemented with 1% penicillin/streptomycin (VSMCs) and at a multiplicity of infection of 500 in serum-free DMEM:F12 supplemented with 1% penicillin/streptomycin (mAECs). After infection, cells were treated as follows: primary rat VSMCs were maintained with 20% FBS in DMEM, E19P were maintained for 24 hours with DMEM supplemented with mitogen-free insulin-transferrin-selenium media (Invitrogen), human VSMCs were maintained for 24 hours with 0.2% FBS in M199, and mAECs were maintained for 24 hours with DMEM:F12 supplemented with 10% FBS, 0.1 mg/mL heparin and 50 µg/ml of ECGF. For platelet-derived growth factor-BB (PDGF-BB) stimulation experiments, E19P cells were starved during 72 hours with mitogen-free insulin-transferrin-selenium/DMEM, and human VSMCs were starved during 48 hours with 0.2% FBS/M199. To induce cell cycle reentry, serum-starved E19P cells and human VSMCs were stimulated with 10 ng/mL of rat PDGF-BB (Sigma) and 20 ng/mL of human PDGF-BB (R&D Systems, Minneapolis), respectively, and then harvested at different times for chromatin immunoprecipitation (ChIP), quantitative real-time PCR (qPCR) or proliferation assays (see below). When indicated, cells were incubated with the following inhibitors during the last hour of serum starvation and throughout the period of PDGF-BB stimulation: 5 µM U0126 (MEK inhibitor, Promega, Madison, Wisconsin), 5 µM AKT inhibitor X (Calbiochem, EMD Chemicals, Inc., Gibbstown, NJ), or 10 µM SB203580 (p38-MAPK inhibitor, Calbiochem, EMD Chemicals).

**Chromatin immunoprecipitation (ChIP) assay.** To quantify the in vivo recruitment of NF-Y to the *CCNB1* promoter, VSMCs (8x10<sup>6</sup> cells) were fixed by supplementing the medium with formaldehyde (1% final concentration, 10 minutes). Cells were extensively washed with ice-cold phosphate-buffered saline and then lysed for 5 minutes in L1 buffer (50 mM Tris, pH 8.0, 2 mM EDTA, 0.1% NP-40, 10% glycerol) supplemented with protease inhibitors (Complete Protease Inhibitor Cocktail, Roche Applied Science, Indianapolis, IN). Nuclei were collected at 3,000 rpm in a microfuge and resuspended in

L2 buffer (50 mM Tris, pH 8.0, 1% SDS, 5 mM EDTA). Chromatin was sheared by sonication using a Bioruptor (Diagenode, Liege, Belgium), centrifuged to pellet debris, and diluted 10 times in 0.5% NP-40/0.2 M NaCl/0.5 mM EDTA/50 mM Tris, pH 8.0. Immunoprecipitation with 3 µg of polyclonal anti-NF-YA or isotype IgG control antibody (sc-10779X and sc-2027 respectively, Santa Cruz Biotechnology) was performed overnight at 4°C. Immune complexes were collected with salmon sperm DNA-saturated protein A, washed three times with high-salt washing buffer (20 mM Tris, pH 8.0, 0.1% SDS, 1% NP-40, 2 mM EDTA, 500 mM NaCl), two times with a 0.5 M LiCl buffer, and three times with low-salt TE buffer (5 minutes each wash). Immune complexes were extracted in TE containing 2% SDS and protein and DNA cross-links were reverted by heating at 65°C for 6 hours. DNA was extracted using QIAquick PCR purification kit (Qiagen, Valencia, CA). Approximately 1/20 of the immunoprecipitated DNA was used in each PCR reaction. The following primers were designed using the Autoprime software ([www.autoprime.de](http://www.autoprime.de)) (sequence from 5' to 3'):

Rat *CCNB1* (Melting temperature: 67°C):

Forward: GCTCTGCCATTTATCATCACT

Reverse: TGA CTGCCAAGCAAGGAAGC

Human *CCNB1* (Melting temperature: 72°C):

Forward: CGATCGCCCTGGAAACGCATT

Reverse: CCAGCAGAAACCAACAGCCGT

Each experimental condition was analyzed in triplicate. Results were normalized using the isotype IgG control and the  $\Delta\Delta$  cycle threshold method and are expressed relative to control group (defined as 1).

**Quantitative PCR (qPCR).** Total RNA was isolated from VSMCs using Qiazol (Qiagen). RNA was quantified by spectrophotometry at 260nm and its purity was assessed by the A260nm/A280nm ratio. RNA integrity was verified by separation on ethidium bromide-stained 1% agarose gels. RNA (0.5 to 2µg) from VSMCs was retrotranscribed using the High Capacity cDNA Reverse Transcription Kit (Applied Biosystems, Carlsbad, CA). qPCR was performed using SYBR Green PCR Master mix (Applied Biosystems) and the following primers (sequence from 5' to 3'):

Rat *NF-YA* (Melting temperature: 60 °C):

Forward: GGAGCCTCTGATTGGGTTTC

Reverse: GCCACGTTGTGTCCTGAAG

Rat *CCNB1* (Melting temperature: 58 °C):

Forward: ATGCAGCACCTGGCTAAGAAC  
Reverse: CATGCTTAGATGTTGCATACTTGT

Rat *18S* (Melting temperature: 60 °C):

Forward: CGGCTACCACATCCAAGGAA  
Reverse: AGCTGGAATTACCGCGGC

Human *CCNB1* (Melting temperature: 60 °C):

Forward: AGCTGCTGCCTGGTGAAGAG  
Reverse: GCCATGTTGATCTTCGCCTTA

Human *HPRT1* (Melting temperature: 60 °C):

Forward: AATTGACACTGGCAAACAATGC  
Reverse: ATGGTCAAGGTTCGCAAGCTT

qPCR results were normalized using the housekeeping genes 18S (rat studies) and HPRT1 (human studies) and the comparative Ct method.

**Proliferation assays.** For the experiments of **Fig.3C**, primary rat VSMCs asynchronously growing in the presence of 20% FBS were infected with Ad-GFP or Ad-GFP-NF-YAdn (see above) and incubated with 50  $\mu$ M 5-bromo-2'-deoxyuridine (BrdU) (Sigma) for 16 hours. The percentage of BrdU-immunoreactive cells was determined in infected cells (GFP-positive). For the rest of proliferation assays, cells were incubated with 50  $\mu$ M BrdU during the last 2 hours (**Fig.2A, B**) or 24 hours (**Fig.2C, 3D**) of PDGF-BB stimulation. Cells were fixed for 30 minutes with 4% paraformaldehyde/PBS, permeabilized with 0.5% Triton X-100/2 M HCl, washed extensively with sodium borate buffer (pH 8.5), and incubated with a rabbit polyclonal anti-GFP antibody (1/500, A6455, Invitrogen). Next, cells were incubated with mouse monoclonal anti-BrdU antibody (1/200, 11-286-c100, clone MoBu-1, Exbio, Vestec, Czech Republic) followed by a biotinylated goat anti-mouse secondary antibody (BA-9200, Vector Labs, Burlingame, CA), Cy3-conjugated streptavidin (016-160-084, Jackson ImmunoResearch, Suffolk, UK) and Alexa Fluor 488-conjugated goat anti-rabbit secondary antibody (A11034, Molecular Probes, Invitrogen). Nuclei were stained with Hoechst (1/1000, Sigma) for total cell count, and coverslips were mounted with slow-fade gold antifade reagent (Invitrogen) and analyzed in an Axiovert 200M fluorescent microscope (Zeiss, Germany). For experiments of **Supplemental Fig. IB**, mAECs were starved in DMEM:F12 for 48 hours. To induced cell cycle reentry, mAECs were stimulated with

DMEM:F12 supplemented with 10% FBS, 0.1 mg/mL heparin and 50 µg/ml ECGF for 24 hours. mAECs were incubated with 50 µM BrdU during the last 24 hours. The percentage of BrdU-immunoreactive cells was determined in infected cells (GFP-positive) as BrdU-APC-positive cells using the BrdU flow kit (557892, Becton Dickinson Pharmigen).

**In vitro apoptosis assays.** VSMCs and mAECs were infected with adenoviral vectors as described above. Cells were grown in the presence of 10% FBS, 0.1 mg/mL heparin and 50 µg/ml ECGF (mAECs, **Supplemental Fig. IB**) or 20% FBS (rat VSMCs, **Supplemental Fig. IIIA**) and apoptosis was analyzed by supravital incubation with 0.003% propidium iodide as described.<sup>13</sup>

**Western blot.** Cytoplasmic and nuclear lysates were prepared as described.<sup>9</sup> Lysates (50 µg protein) were separated by SDS-PAGE and transferred onto Immobilon-P membranes (Millipore Corporation, Billerica, MA). Membranes were blocked in 4% dry milk and incubated with primary antibodies (anti-NF-YA, 1/1000, 200-401-100, Rockland, Gilbertsville, Pensilvania; anti-lamin A/C, 1/300, sc-6215, Santa Cruz Biotechnology). Secondary horseradish peroxidase-coupled anti-isotype-specific antibodies (Santa Cruz Biotechnology) were used for detection with enhanced chemiluminescence reagent (ECL Plus; GE Healthcare, UK).

**Statistical analysis.** Results are expressed as mean±SEM and analyzed using SPSS (SPSS Inc., Chicago, IL) and GraphPad-Prism (GraphPad Software, LaJolla, CA). Statistical significance was considered when  $p < 0.05$ , as determined by paired 2-sided Student's *t* test (2 experimental groups) and one-way or two-way ANOVA followed by Bonferroni's or Dunnett's test (>2 experimental groups).

## REFERENCES

1. Meir KS, Leitersdorf E. Atherosclerosis in the apolipoprotein-E-deficient mouse: A decade of progress. *Arterioscler Thromb Vasc Biol.* 2004;24:1006-1014
2. Indolfi C, Avvedimento EV, Rapacciuolo A, Di Lorenzo E, Esposito G, Stabile E, Feliciello A, Mele E, Giuliano P, Condorelli G, Chiariello M. Inhibition of cellular ras prevents smooth muscle cell proliferation after vascular injury in vivo. *Nat Med.* 1995;1:541-545
3. Luo J, Deng ZL, Luo X, Tang N, Song WX, Chen J, Sharff KA, Luu HH, Haydon RC, Kinzler KW, Vogelstein B, He TC. A protocol for rapid generation of recombinant adenoviruses using the adeasy system. *Nat Protoc.* 2007;2:1236-1247
4. Mantovani R, Li XY, Pessara U, Hooft van Huisduijnen R, Benoist C, Mathis D. Dominant negative analogs of NF- $\kappa$ B. *J Biol Chem.* 1994;269:20340-20346
5. Bauriedel G, Schluckebier S, Hutter R, Welsch U, Kandolf R, Luderitz B, Prescott MF. Apoptosis in restenosis versus stable-angina atherosclerosis: Implications for the pathogenesis of restenosis. *Arteriosclerosis, thrombosis, and vascular biology.* 1998;18:1132-1139
6. García-Ramírez M, Martínez-González J, Juan-Babot JO, Rodríguez C, Badimón L. Transcription factor SOX18 is expressed in human coronary atherosclerotic lesions and regulates DNA synthesis and vascular cell growth. *Arterioscler Thromb Vasc Biol.* 2005;25:2398-2403
7. Ivorra C, Kubicek M, González JM, Sanz-González SM, Álvarez-Barrientos A, O'Connor JE, Burke B, Andrés V. A mechanism of AP-1 suppression through interaction of c-fos with lamin A/C. *Genes Dev.* 2006;20:307-320
8. Sanz-González SM, Melero-Fernandez de Mera R, Malek NP, Andrés V. Atheroma development in apolipoprotein e-null mice is not regulated by phosphorylation of p27(kip1) on threonine 187. *J Cell Biochem.* 2006;97:735-743
9. González JM, Navarro-Puche A, Casar B, Crespo P, Andrés V. Fast regulation of AP-1 activity through interaction of lamin A/C, ERK1/2, and c-fos at the nuclear envelope. *J Cell Biol.* 2008;183:653-666

10. Ruiz-Ortega M, Lorenzo O, Rupérez M, König S, Wittig B, Egido J. Angiotensin II activates nuclear transcription factor kappaB through AT(1) and AT(2) in vascular smooth muscle cells: Molecular mechanisms. *Circ Res.* 2000;86:1266-1272
11. Esteban V, Méndez-Barbero N, Jiménez-Borreguero LJ, Roque M, Novensa L, García-Redondo AB, Salaices M, Vila L, Arbones ML, Campanero MR, Redondo JM. Regulator of calcineurin 1 mediates pathological vascular wall remodeling. *J Exp Med.* 2011;208:2125-2139
12. Martínez-González J, Badimón L. Human and porcine smooth muscle cells share similar proliferation dependence on the mevalonate pathway: Implication for in vivo interventions in the porcine model. *Eur J Clin Invest.* 1996;26:1023-1032
13. Zamai L, Canonico B, Luchetti F, Ferri P, Melloni E, Guidotti L, Cappellini A, Cutroneo G, Vitale M, Papa S. Supravital exposure to propidium iodide identifies apoptosis on adherent cells. *Cytometry.* 2001;44:57-64